TAO, Vol. 13, No. 4, 469-498, December 2002

The Biennial Oscillations in Taiwan

Mong-Ming Lu[1,*]

(Manuscript received 7 March 2001, in final form 16 October 2002)

ABSTRACT

A spectral analysis and a method using the conditional probability approach are performed on 41-year (1958-1998) monthly station pressure, temperature and precipitation data in Taiwan to identify the local climate biennial oscillation (BO) signal. Two Taiwan BO modes are identified in this study. One is the November-December (ND) temperature and the other is the January-February (JF) precipitation.

The relationship between Taiwan BO modes and certain known BO phenomena is investigated for clarifying the robustness of the modes. The ND temperature mode is found to be associated with the BO in the sea surface temperature (SST) of the South China Sea (SCS) and the BO mode of ENSO. The JF precipitation mode is also associated with the BO mode of ENSO with the enhancement of the warm anomalies of the SCS SSTs. The JF precipitation mode is observed clearly after 1982, but cannot be identified before 1982. The ND temperature mode is observed more clearly before 1982. The amplitude of fluctuation in the ND temperature is relatively small when the rhythm of the biennial fluctuation is clearer. When the biennial fluctuation is smeared by low-frequency signal after the late-1970s, the amplitude becomes larger. The effect is completely the opposite for the BO modes of JF precipitation.

The discrepancy between the BO modes of ND temperature and JF precipitation are examples showing how the local climate of Taiwan can be influenced by low-frequency variations of tropical and extratropical climate systems. The rapid warm trend of SCS SSTs and Eurasia continent since the late-1970s can enhance the BO signal of JF precipitation but weaken the signal of ND temperature.

(Key words: Biennial Oscillations, Taiwan climate, Regional climate variations)

[1]Central Weather Bureau, Taipei, Taiwan ROC

* *Corresponding author address*: Dr. Mong-Ming Lu, Central,Weather Bureau, 64 Kung-Yuan Rd. Taipei, Taiwan, 100 ROC; E-Mail: lu@rdc.cwb.gov.tw

1. INTRODUCTION

Tropospheric quasi-biennial oscillation (TBO) has received considerable attention in the past half century. The most well-known phenomenon that fluctuates in a biennial time scale is the Southern Oscillation (Troup 1965; Yasunari 1987; Rasmusson et al. 1990; Barnett 1991; Ropelewski et al. 1992; Tomita and Yasunari 1993). The temporal variation of the Southern Oscillation (SO) can be decomposed into three major components: the quasi-biennial oscillation (BO), the annual cycle and the low-frequency fluctuation (Barnett 1991; Ropelewski et al. 1992). Strong BO mode was found in the equatorial Indian Ocean and the West Pacific. The BO mode of the Indian monsoon system was documented by Terray (1995). After analyzing multiyear (1900-1970) sea level pressure (SLP), sea surface temperature (SST), air temperature and rainfall data in the Indian sector, he found two major components of monsoon variability: the biennial mode and the low-frequency mode. The biennial mode is best represented by the southwest-northeast gradient of SLP anomalies. In addition to the tropical phenomenon, a midlatitude BO in the Southern Hemisphere was clearly identified by Trenberth (1975) in SLP and SST fields. He found that the SLP BO corresponds to the fluctuations of the midlatitude wavenumber-3 planetary wave. In East Asia, Shen and Lau (1995) found a BO mode in East Asian summer monsoon rainfall. More recently, Tomita and Yasunari (1996) identified the BO in SST of the South China Sea (SCS). They pointed out that the phase transition of the SCS BO leads the transition of the BO mode of ENSO by about half a year. Based on the fact that the SCS BO mode is highly modulated by the East Asian northeast winter monsoon, they suggested that the tropical-extratropical interaction might play an essential role in the BO of the Asian monsoon and ENSO system.

TBO of a different kind was pointed out in Meehl (1987). He showed that in the tropics, strong Australian monsoon tends to follow strong Indian monsoon. The Indian monsoon rainfall fluctuates in biennial time scale. Therefore, the tropical Asian-Australian (A-A) monsoon system fluctuates biennially in a coherent way. He suspected that such oscillation might have resulted from hemispherical scale coupled land-atmosphere-ocean interactions (Meehl 1997). On the other hand, Chang and Li (2000) showed that the biennial oscillations of the tropical A-A monsoon system is an inherent phenomenon resulting from the interactions between A-A summer and winter monsoon and the tropical Indian and Pacific Oceans. Differing from Meehl's conceptual model, Chang and Li showed that tropical-extratropical interaction and the interaction with the eastern Pacific are not necessary to produce a BO in the A-A monsoon region.

The Taiwan local climate system belongs to the East Asian monsoon system, which is connected with the tropical A-A monsoon system. Therefore, understanding TBO and its relationship with Taiwan climate variability is of profound importance for local climate prediction. Lu (2000, p.100) found that in the warm phase of ENSO, Taiwan tends to be warmer than normal during the winter and the following spring. The warm situation in Taiwan is more clearly observed for the BO mode of ENSO compared with the low-frequency mode. The anomalous southerly winds over the SCS and the Philippine Sea are associated with the warm local climate. Wang et al. (2000) pointed out that the impact of ENSO on East Asian climate can be made through a Pacific-East Asian teleconnection pattern. When a strong warm or cold ENSO event matures, anomalous winds over the western North Pacific can develop rapidly in

late fall of the year and persist until the following spring or early summer. The anomalous winds are part of the anomalous Philippine Sea anticyclone, which results from a Rossby-wave response to suppressed convective heating induced by both the in situ ocean surface cooling and the subsidence forced remotely by the central Pacific warming. These results suggest that probably only in certain selective situations of ENSO can the impact of large-scale abnormal conditions on Taiwan climate be identified with confidence. The current study is a first-step in the author's attempt to identify useful phenomena for monitoring and predicting Taiwan local climate variability.

In this study, we will try to answer two questions:

- Can BO be identified in Taiwan station data?
- If BO can be identified, to what degree is it related with certain known BO phenomena such as SOI, Indian and extratropical Australian monsoons?

This paper is organized as follows. The data and methodology are described on Section 2. The procedure for determining the BO in Taiwan climate is explained in Section 3. The relationship between Taiwan BO and the BO mode of SOI, Indian Monsoon and Australian Monsoon are documented in Section 4. Discussion and interpretation are given in Section 5. Conclusions are drawn in the last section.

2. DATA AND METHODOLOGY

2.1 Data

Three sets of 41-year (1958-1998) data are used in this study. The first set is Taiwan station data. The stations are listed in Table 1. The monthly temperature, precipitation and station pressure data in the 20 stations are used. The second data set is the SLP field in the NCEP/NCAR Reanalysis (Kalnay et al. 1996) monthly grid (2.5°x2.5°) data. The third set is Kaplan extended SST anomaly data (http://ingrid.ldeo.columbia.edu/ SOURCES/.KAPLAN/. EXTENDED/.ssta). Both NCEP/NCAR reanalysis and the SST anomaly data were obtained from the data library of the International Research Institute for climate prediction (IRI).

2.2 BO Indices

Four BO indices are defined. The purposes of defining these indices are, on the one hand, to simplify the comparison between Taiwan and other BO signal and, on the other hand, to incorporate some of the indices into the operational climate monitoring system of the Central Weather Bureau (CWB) of Taiwan. It should be stressed that, besides the conventional ENSO indices, the BO indices are defined according to the published results with further simplifications made by the author of the present study. Although they may not be the most suitable indices for capturing BO, they are ones that already show convincing evidence of the oscillations and can be verified using easily accessible grid data sets.

(i) Indian Monsoon BO index (IMBO)

Following the results of Terray (1995), we define an Indian monsoon BO index (IMBO)

Table1. Characteristics of the 20 Taiwan stations used in this study.

Station ID	Stations Name	Latitude	Longitude	Altitude (m)
695	Pengchiayu	25°38'	122°04'	104.6
694	Keelung	25°08'	121°44'	27.7
690	Tanshui	25°10'	121°26'	23.0
691	Anpu	25°11'	121°31'	827.1
693	Chutzehu	25°10'	121°32'	607.6
692	Taipei	25°02'	121°30'	7.1
757	Hsinchu	24°49'	121°00'	28.9
765	Jiyuehtan	23°53'	120°54'	1014.8
749	Taichung	24°09'	120°41'	85.3
753	Alishan	23°31'	120°48'	2415.9
741	Tainan	23°00'	120°12'	14.7
744	Kaohsiung	22°34'	120°18'	3.1
759	Hengchun	22°00'	120°44'	24.1
735	Penghu	23°34'	119°33'	11.4
708	Ilan	24°46'	121°45'	8.0
699	Hualien	23°59'	121°36'	19.1
761	Chengkung	23°06'	121°22'	37.8
766	Taitung	22°45'	121°09'	9.0
754	Tawu	22°21'	120°54'	8.9
762	Lanyu	22°02'	121°33'	305.1

based on the southwest-northeast SLP anomaly gradient. IMBO is the arithmetic difference of the normalized anomalies of the SLP at two grid points, (17.5°N, 90°E) and (2.5°S, 52.5°E) (the value at the later point subtracted from the former). These two points are determined according to Fig. 1b of Terray (1995), which shows the spatial pattern of the rotated EOF2 of SLP. The EOF2 describes a southwest-northeast SLP anomaly gradient. The power spectra of its principal component (Fig. 4 in his paper) show clear biennial signal. It should be noted that the BO signal is clearest during the period III in his paper which is May 1947 - December 1970.

(ii) Australian Monsoon BO index (AMBO)

If we separate the Australian monsoon into tropical and extratropical components, the extratropical Australian monsoon is part of "the rearrangement of the long wave from summer to winter" (Trenberth 1975, p.57). We find that the BO mode is more clearly documented in

(a)

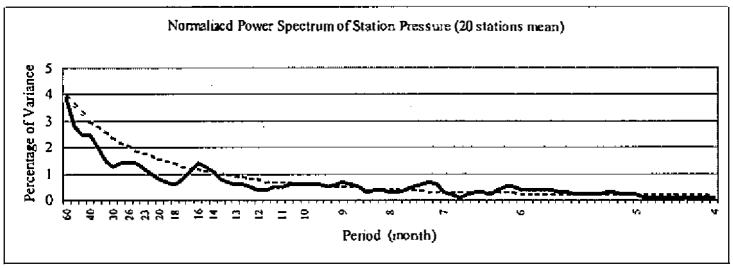

(b)

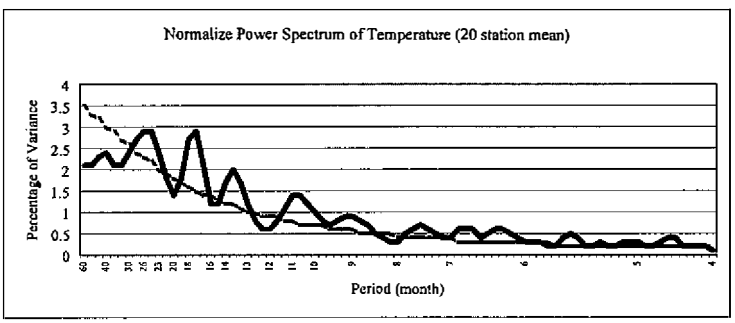

(c)

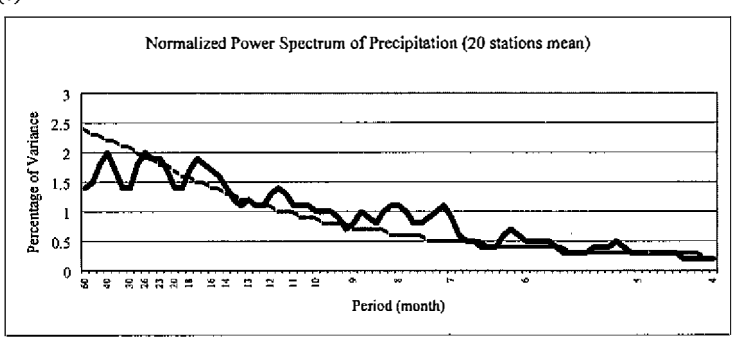

Fig. 1. Normalized power spectra for Taiwan (a) station pressure, (b) temperature and (c) precipitation. The dashed lines are the null hypothesis of red noise.

the extratropics. Trenberth (1975) performed EOF analysis on the monthly SLP in the Australiasian area and on the SST in the Tasman Sea. He showed by performing power spectrum analysis on the principal components that the EOF2 of SLP has the most significant BO signal (Fig. 8 in his paper). The EOF2 pattern shows northwest-southeast SLP anomaly gradient with the centers of action near the stations of Hobart (43°S, 147.5°E) and Catham Islands (43°S, 176°W) (Trenberth 1980). This BO mode was found to be part of the fluctuations of

the planetary-scale wave with wavenumber 3 in the Southern Hemisphere. According to Trenberth's results, we define an Australian Monsoon BO index (AMBO) by calculating the arithmetical difference of the normalized SLP anomalies at two grid points: (40°S, 150°E) and (50°S, 180°E). These two grid points are determined based on the EOF2 of SLP shown in the Fig. 4.2 of Trenberth (1975).

(iii) South China Sea SST index (SCSS and SCSN)

It has been shown in Shen and Lau (1995) and Tomita and Yasunari (1996) that the percentage of BO with respect to the total variance of interannual fluctuations of SST is relatively high in the marginal seas between Asia and Australia. The seas include the East China Sea, the South China Sea, the Timor Sea, the Arafura Sea and the Coral Sea. The signal in the SCS and the Timor Sea is particularly strong. Among them, we are most interested in the relationship between Taiwan local climate and SCS SST BO. Two SCS indices, SCSS and SCSN, are defined for this purpose. SCSS is the normalized SST anomalies averaged over the area of 105-115°E and 5-10°N. SCSN is over the area of 110-120°E and 10-20°N. The SCS is separated into two because of the possible difference between the BO signal in the tropics and in the latitudes slightly higher. The strong BO signal over the SCS demonstrated in Ropelewski et al. (1992) is mainly near the equatorial region.

(iv) ENSO BO index (Nino4, SOI, DARSLP, TAHSLP)

The ENSO events can be classified into two types of biennial and low-frequency (Barnett 1991; Tomita and Yasunari 1993) time scales based on the duration of the same sign SST anomaly. It can be found in many literatures that the variability in the Asian Monsoon system and the SST and circulation over the Pacific are correlated in a biennial time scale (Meehl 1987, 1993; Yasunari 1990; Ropelewski et al. 1992). Four ENSO indices, namely Nino4, SOI, DARSLP and TAHSLP, are used in the present study. The Nino4 index is the SST averaged over the area of 160°E-150°W and 5°S -5°N. The SOI, TAHSLP and DARSLP are obtained from Climate Prediction Center of NOAA (http://www.cpc.noaa.gov). SOI is computed from the normalized difference between TAHSLP and DARSLP, the standardized SLP anomaly at Tahiti and Darwin.

2.3 Methodology

The analysis procedure is as follows. We first identify the Taiwan BO by analyzing station data by two methods: the conventional spectrum analysis method and the conditional probability approach. The spectrum analysis is performed using IMSL package. The seasonal cycle is removed from the time series by subtracting its 41-year average from the monthly data before calculating the power spectrum. The anomalies are normalized with respect to the monthly standard deviation for each month after the seasonal cycle is removed. The linear trends of the normalized anomalies are also removed before computing the power spectral density. It should be noted that the spectrum analysis is applied to the entire time series of the 41 years of monthly data without selecting any specific season.

The conditional probability approach is adopted for two reasons. First, the seasonal and regional dependence of Taiwan BO signal are important. The second reason is that it is necessary to deal with individual cases for identifying the discontinuous oscillation-like signal of Taiwan BOs. In the conditional probability approach, we first transfer the monthly data to bimonthly for reducing climate noise. Then, we compute the percentile ranks (PRs) of the bimonthly data. Finally, we count the frequencies of above normal (PR > 70), normal ($30 \leq$ PR ≤ 70) and below normal (PR < 30) before and after the control years. The control years are the selected "abnormal" years in which the category is either above or below normal. If the frequency clearly inclines to the opposite category of the control one, it means that the time series possesses a BO tendency. The conditional probability approach is applied to the data of each 20 stations. An example of this approach will be given in Section 3.

After identifying Taiwan BO signal, we select some strong BO events and then use the composite method to illustrate possible relationship between Taiwan and other BO signals.

3. TAIWAN BO

3.1 Power Spectrum Analysis

The power spectra of the monthly station pressure, temperature and precipitation are calculated for 20 Taiwan stations (Table 1) individually as well as for their averages. The overall result can be represented by the percentage of the variance explained at each frequency interval (Figs. 1a-c) computed from the average spectra of 20 stations. The spectral window width used here is 180 months. The variance contributed by the fluctuations with periods in the range of 16-36 months, is about 18.0% of the total variance in station pressure, 30.4% in temperature and 25.1% in precipitation. The BO scale spectral peaks in temperature (Fig. 1b) and precipitation (Fig. 1c) are above the background red noise. Despite the high climate noise level, represented by the fluctuations with the periods less than one year, the fluctuations of temperature and precipitation in the BO scale can be separated from other kinds of fluctuations.

3.2 Conditional Probability Approach

The BO signal is further extracted using a conditional probability approach. The seasonal and geographical dependency of Taiwan BO can be clarified using this approach. An inherent assumption of this approach is that BO is phase-locked with seasonal cycles, which is a common feature of BO, as many studies have suggested (e.g., Meehl 1987 and the reference therein). It has been shown in theories that TBO bears a modulation relation to the annual cycle forcing (e.g., Brier 1978, Nicholls 1978). We will only discuss the BO in temperature and precipitation in the rest of this paper because the power spectrum of station pressure does not show any promising signal of interest (Fig. 1a).

We first transform the 41-year bimonthly temperature and precipitation data to PR. It should be kept in mind that in this study we use the bimonthly data to represent the "seasons". The symbols of the "seasons" are "JF" for Jan-Feb, "MA" for Mar-Apr, "MJ" for May-June, and etc. Then, we classify the data at each station into three categories. For temperature data,

the warm category means PR larger than 70, the cold means PR less than 30, and normal otherwise. For precipitation, wet means PR larger than 70, dry for PR less than 30, and normal otherwise. Then, we simply count the number of years in each category before or after the control years. If the result shows that the year before or after the control years has a strong tendency of being in the opposite category with respect to the control one, the BO signal is then identified. We have checked the temperature and precipitation data for all seasons. Given the total sample size as 41, there are 12 members in each abnormal category and 16 members in normal. If the number of years in the opposite category is larger than 50% of the sample size, which is 6 in this study, and the number of years in the same category is less than 3, then a BO signal is identified.

We find that the BO signal in temperature can only be identified in early winter: the ND. Figure 2 shows the counts for the number of years in different categories before and after the warm or cold years. The length of the bars reflects the number of the count. Using station 695 (Pengchiayu) as an example, Fig. 2a shows that before the warm NDs of station 695, there are 6 out of 12 NDs (50%) in the cold category and 2 out of 12 (16%) in the warm category. Figure 2b shows after the warm NDs of station 695, there are also 6 out 12 (50%) in the cold category and 2 out of 12 (16%) in the warm category. Figure 2c shows before the cold NDs of station 695, there is only 1 ND out of 12 (8%) in cold category, while 6 out of 12 (50%) in warm category. Figure 2d shows after the cold NDs of station 695, there is 1 (8%) cold ND but 7 (58%) warm NDs. These results suggest that the ND temperature at station 695 oscillates quasi-biennially. It can be noted by comparing Figs. 2a-d that, in terms of the number of stations satisfying the category opposite to the control one, the BO signal is particularly strong in Fig. 2c. 7 out of the 20 stations satisfy the BO criterion. In contrast to other seasons in which the BO criterion cannot even be satisfied by one single station, the BO signal shown in Fig. 2c is outstanding.

The results of Taiwan BOs identified using the conditional probability approach is summarized in Table 2. Alphabetic symbols are used to represent different types of BO. For example, if a BO criterion such as "the year before a warm year tends to be a cold one" is satisfied, then the symbol "A" is marked. The symbols are remarked in the NOTE box in Table 2. We have just seen the example of the ND temperature of the station 695. The BO criterion is actually satisfied in all conditions of using either warm or cold years as the reference years at that particular station. Therefore, the symbol "ABCD" is marked in the box of ND temperature of station 695.

Table 2 shows the temperature BO signal can be identified only in ND. There are 9 out of 20 stations showing some signal. "C" is the most common type of BO, which means before a cold ND the chance of a warm ND in the previous year is high. Type "B", which means it tends to be a cold ND after a warm ND, can only be identified in 3 stations (695, 690, 759). It is interesting to see that the BO signal is found in all of the small island stations (695, 735, 762).

The precipitation BO signal is found in all seasons except the transition ones of MA and SO. The precipitation BO signal is strongest in JF, though it can only be identified on the western side of the Central Mountain Range as shown in Table 2. Weak BO signal of MJ (mei-yu season) precipitation can be identified in northern Taiwan. Two mountain stations in northern Taiwan (691, 693) show BO in JA. The weak ND precipitation BO signal does not show a

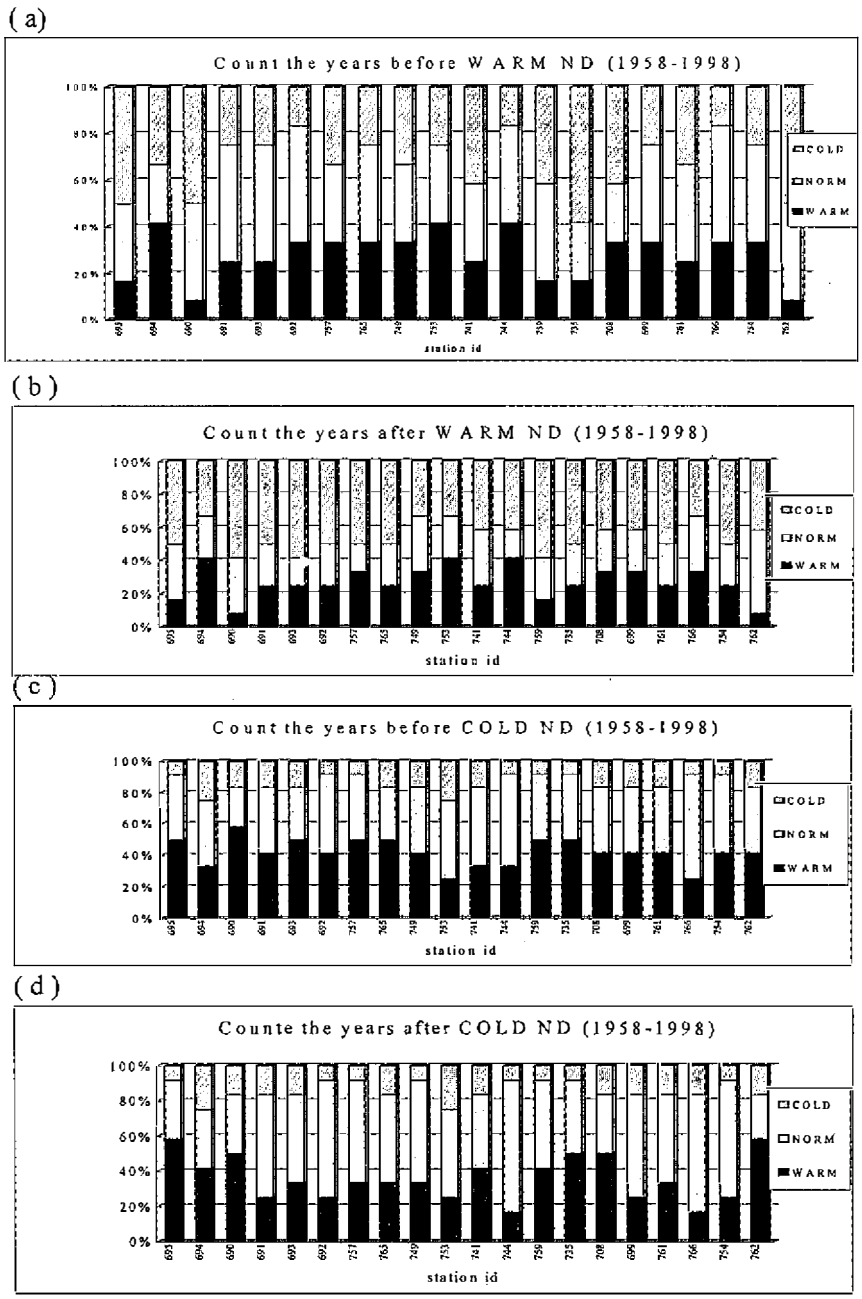

Fig. 2. The percentage of cases in three different categories of Taiwan ND temperature for the cases (a) before the warm years, (b) after the warm years, (c) before the cold years and (d) after the cold years. The dark shaded portion represents the warm category and the light shaded portion represents the cold category.

Table 2. A summary of Taiwan BO types.

STATION ID/ NAME	BIENNIAL OSCILLATINO TYPE				
	Temperature	Precipitation			
	ND	JF	MJ	JA	ND
695/ Pengchiayu	ABCD		Y		
694/ Keelung					
690/ Tanshui	ABCD	WY	W		
691/ Anpu			XY	Y	Y
693/ Chutzehu	C		WXYZ	WXYZ	Y
692/ Taipei		Z			
757/ Hsinchu	C	X			
765/ Jiyuehtan	C	XZ			
749/ Taichung		XY			
753/ Alishan		X			
741/ Tainan		WXYZ		X	
744/ Kaohsiung					Z
759/ Hengchun	BC				
735/ Penghu	ACD	X			Y
708/ Ilan	D			Y	
699/ Hualien					
761/ Chengkung					Y
766/ Taitung					Z
754/ Tawu					
762/ Lanyu	AD				
NOTE: Type Symbol	A: Cold - Warm* B: Warm* - Cold C: Warm - Cold* D: Cold* - Warm *: reference category		W: Dry - Wet* X: Wet* - Dry Y: Wet - Dry* Z: Dry* - Wet		

clear geographical pattern. We will only discuss the JF precipitation signal in the rest of this paper because the signals in other seasons are limited to only a few stations.

The ND temperature and JF precipitation signals summarized in Table 2 are subsequently verified against the time series of station data of which the signal is identifiable. Figure 3a shows the time series of the normalized ND temperature anomalies for 7 stations with BO type "C" (before a cold year it tends to be a warm year). The BO can be immediately recognized in Fig. 3a in which there are two regimes of the oscillations. Before 1977, the ND temperature clearly fluctuates in a time scale of about two years. The time scale of the fluctuations extends after 1977. The fluctuation amplitude is rather small during the period of 1978-1993, while it

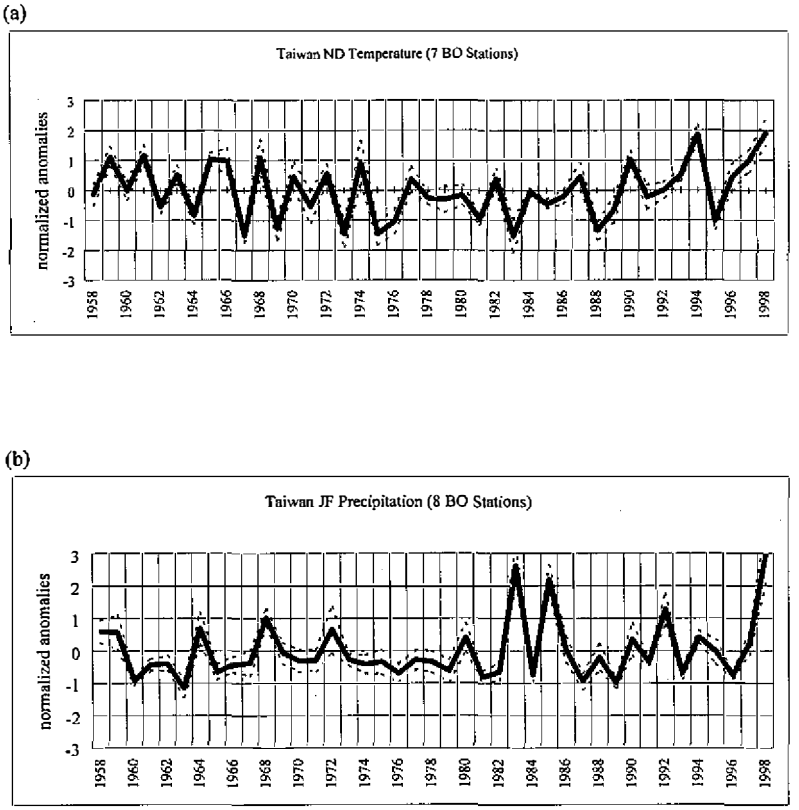

Fig. 3. The time series of the average normalized anomalies of Taiwan (a) Nov-Dec temperature and (b) Jan-Feb precipitation and of 7 and 8 stations in (a) and (b), respectively. See text for description of the stations. Plus and minus one standard deviation is give by the dashed lines.

becomes remarkably large from 1994. The abnormally warm temperature, including three years of continuous positive anomalies starting from 1996, is unique in these 41 years of study.

The time series of the average JF precipitation anomalies for the 8 stations with BO (Table 2) is shown in Fig. 3b. Differing from the ND temperature, the precipitation BO signal is particularly clear during the period of 1979-1994. The abnormally wet years of 1983, 1985 and 1998 are outstanding. Comparing Figs. 3a and b, we find that the ND temperature BO is in general stronger before the late-1970s, while the JF precipitation BO is stronger after the late-1970s. This contrast suggests that different criteria may be required for results in the BO of temperature and precipitation.

3.3 The Seasonality of BO

The seasonal dependency of the BO signals can be illustrated by the comparison of the

percentage variance contributed by the fluctuations with the periods in the ranges of 3-5 years and 2-3 years (Figs. 4 and 5). The period range of 3-5 years is chosen to represent the low-frequency peak in Figs. 1b and c. The percentage variance is computed from the individual power spectrum of the 41-point time series of each particular "season". Figure 4a shows the average result of the 9 stations, with stronger temperature BO signals shown in Table 2. The average result of the 11 stations with weaker BO signals is shown in Fig. 4b. The variance

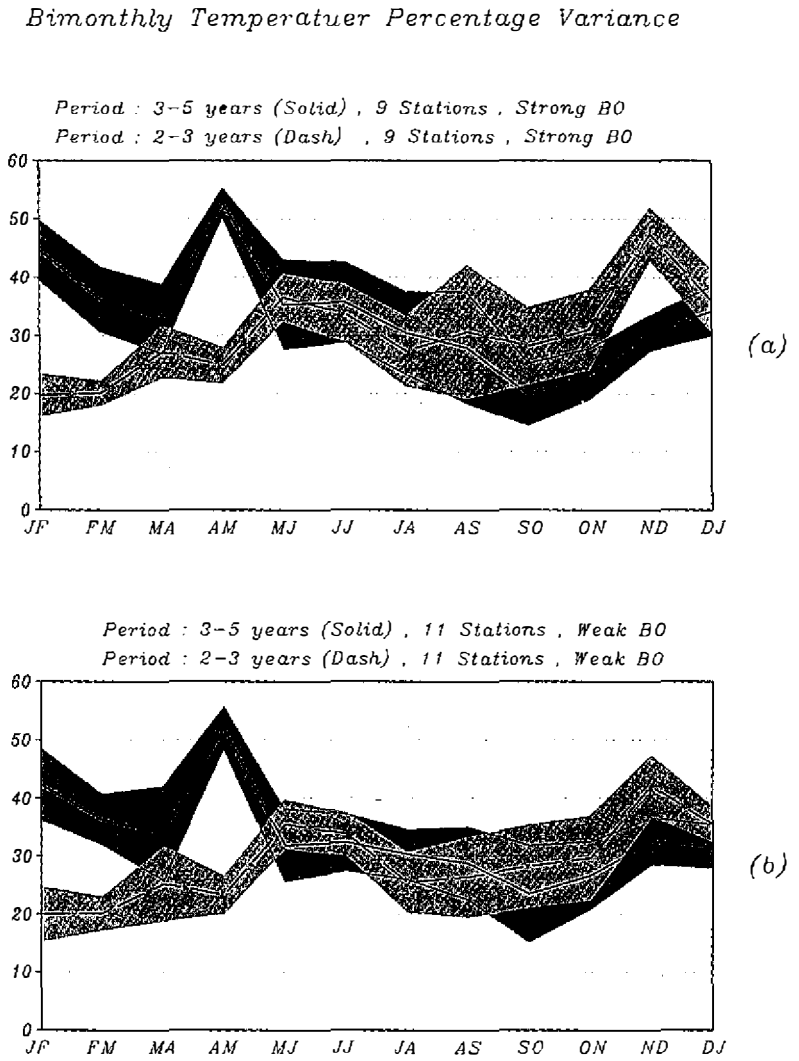

Fig. 4. The annual distribution of the percentage variance explained by two kinds of temperature fluctuations composite for (a) the 9 stations with stronger BO signal and (b) the 11 stations with less BO signal. The fluctuation with the period in the ranges of 2-3 years is light shade (the dashed lines) and in the ranges of 3-5 years is dark (the solid line).

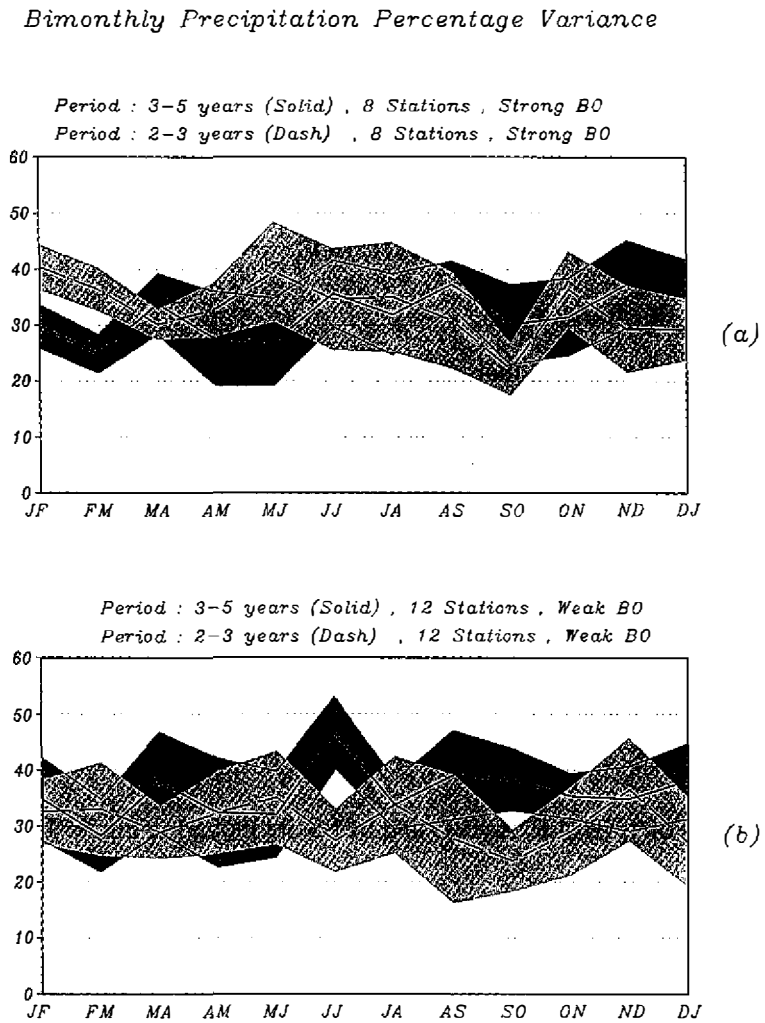

Fig. 5. Same as Fig. 4 but for (a) the 8 stations with stronger precipitation BO signal and (b) the 12 stations with less precipitation BO signal.

contributed by low-frequency fluctuations (periods: 3-5 years) is, on average, larger than by the high-frequency (BO) fluctuations. The contrast is sharper in the earlier portion of the year from January to May, particularly in the season of AM. However, in the season of ND, we observe a different kind of contrast, such as the BO contribution, clearly surpassing the low-frequency part. The contrast in ND is less clear in Fig. 4b, the average of the 11 stations with weaker BO signals.

The comparison of the percentage variance for precipitation is shown in Fig. 5. There is less seasonal dependency in the relative magnitude of the contributions from these two types of fluctuations. However, it is very encouraging to see the only time of the year when the BO contribution surpasses the low-frequency part is JF and FM (Fig. 5a). Another interesting

contrast is the relatively low contribution in MA and SO, in which the BO signal is the weakest (Table 2). Therefore, the percentage variance illustrated in Figs. 4 and 5 supports the findings of Taiwan BO signals summarized in Table 2. Furthermore, it is shown that the BO is a major component in the interannual variations of Taiwan temperature and precipitation in ND and JF, respectively.

4. THE RELATIONSHIP BETWEEN THE BOS

4.1 Evaluating the BO Indices

The percentage of variance that can be explained by the biennial-scale fluctuations in monsoons and ENSO is also examined by computing their power spectra (not shown). The total percentage of the variance contributed by the fluctuations with periods of 12-40 months is about 41.2% in Nino4, 38% in SOI, 37.6% in SCSS, 35.1% in SCSN, 33.6% in DARSLP, 29.3% in TAHSLP, 19.2% in AMBO and 16.8% in IMBO. Four significant spectral peaks are found at the period of 40 months in Nino4, 30 months in TAHSLP, 20 months in AMBO and the period of 12 months in SCSS. Although the SOI has very high percentage of variance in the biennial time scale, its power spectrum does not have any corresponding spectral peak reaching the 5% significance level. As for Nino4, even after filtering out the fluctuations with periods longer than 48 months, it still does not show any isolated spectral peak with a biennial scale period. However, isolated spectral peaks can indeed be identified in the spectra of TAHSLP, AMBO and SCSS. Therefore, we will mainly focus on these three BO indices from now on.

The time series of TAHSLP, AMBO and SCSS are plotted in Fig. 6. The biennial oscilla-

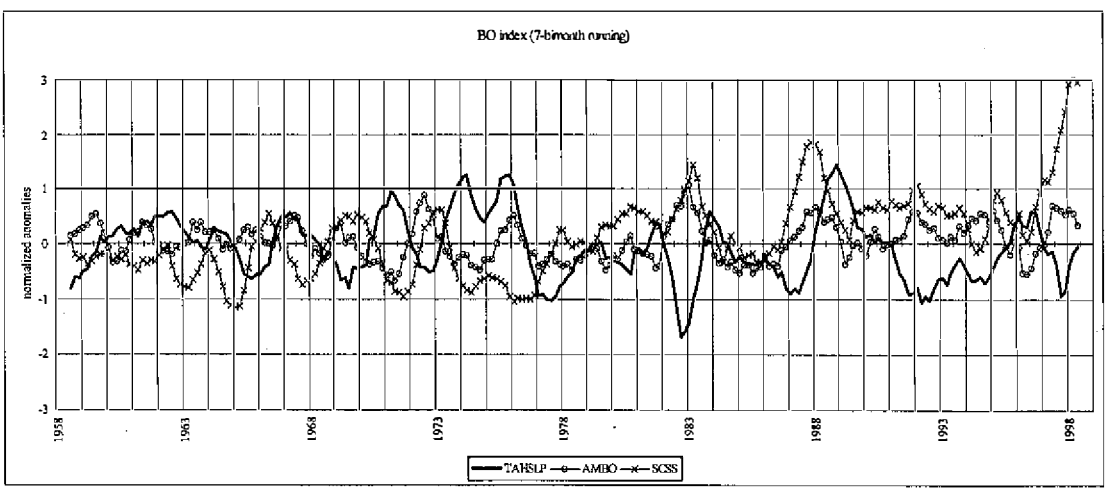

Fig. 6. Time series of the normalized BO indices. The thick solid line is THASLP. The line marked by circles is AMBO and marked by crosses is SCSS. The definition of the BO indices is given in Section 2b.

tions in these three indices can be more clearly identified before, say, 1977 than after. The biennial oscillations of AMBO are quite regular during the period of 1958-1970, but the amplitude of the oscillations is small. During the same period of years, neither TAHSLP nor SCSS shows comparable biennial oscillations. After 1982, the frequency of the interannual variations of both TAHSLP and SCSS became much lower. The biennial oscillations of THASLP are most clearly seen in the years of 1964-1977.

The general relationship between these three indices can be obtained from their correlation coefficients shown in Table 3. The correlation between AMBO and SCSS is the lowest (-0.10) during the period of 1958-1970, which is in sharp contrast to the correlation coefficient of 0.8 in 1978-1989. During the period in which TAHSLP has clear BO (1964-1977), the correlation between TAHSLP and SCSS (-0.49) is larger than in other years, while the correlation between TAHSLP and AMBO is the lowest (-0.14). Therefore, the BOs of TAHSLP and SCSS are possibly associated with each other in 1964-1977, but not correlated with AMBO. On the other hand, the coherent BOs in AMBO and SCSS during 1978-1998 do not oscillate coherently with ENSO.

4.2 Taiwan BO and BO Indices

In this subsection, we examine the possible relationship between Taiwan BO and the BO of TAHSLP, AMBO and SCSS. We have shown that Taiwan BO can be most clearly identified in ND temperature and JF precipitation. After checking the correlations and studying Fig. 6, the author found that the biennial characteristics of the BO indices can be represented by their annual means on the calendar year basis. The correlation coefficients of Taiwan BO parameters and the annual average BO indices during the periods with different BO features

Table 3. The correlation coefficients between the monthly normalized anomalies of TAHSLP, AMBO and SCSS during four different periods. The correlation coefficients with "*" are significant on the 5% level, and with "**" on the 1% level.

		TAHSLP	AMBO	SCSS
TAHSLP	*1958-1970*	1	-0.18	-0.39
	1964-1977	1	-0.14	-0.49*
	1978-1989	1	-0.19	0.08
	1987-1998	1	-0.34	-0.14
AMBO	*1958-1970*		1	-0.1
	1964-1977		1	0.19
	1978-1989		1	0.80**
	1987-1998		1	0.53*
SCSS	*1958-1970*			1
	1964-1977			1
	1978-1989			1
	1987-1998			1

are shown in Table 4. On average, the correlation between Taiwan BO and the BO indices before 1978 is smaller than that after 1978. Before 1978, no correlation coefficient is significant on the 1% level. After 1978, in addition to the correlation coefficient of Taiwan ND temperature and TAHSLP, the correlation coefficient of Taiwan JF precipitation and SCSS is also significant on the 1% level.

It should be noticed that compared to low frequency variability, BO is weak, especially in the time series of ENSO BO indices. Therefore, the correlation analysis here needs to be interpreted with caution because of the contamination of low frequency variability. In other words, the high correlations between Taiwan BO and the other BO indices can be contributed mainly by low frequency variations instead of by variations in biennial time scale. To separate the low frequency variability from BO, we can composite the BO indices based on Taiwan BO events.

Seven cases of ND temperature BO and 8 cases of JF precipitation BO are selected to do the composite. The time span of each case is 17 months. The three reference months are the warm ND (wet JF) as the 9th month, which is also the central month, and the cold ND (dry JF) as the 3rd and 15th months. The cases are selected based on Figs. 3a and b with the stipulation that both of the upper and lower bounds of the anomaly, computed as adding and subtracting the standard deviation to and from the average value respectively, of at least one of the three reference months are larger than 0.5 times of the standard deviation. The 7 cases of the ND temperature BO are: 1962-1964, 1967-1969, 1971-1973, 1973-1975, 1976-1978, 1981-1983 and 1986-1988. The 8 cases of the JF precipitation BO are: 1963-1965, 1967-1969, 1971-1973, 1979-1981, 1982-1984, 1984-1986, 1991-1993, and 1993-1995.

The composite TAHSLP and its standard deviation are shown in Fig. 7a. The symbol ND0 represents the ND in the central reference year, ND+1 represents the ND in the year after the central reference year, and ND-1 represents the ND in the year before the central reference year. In the case of Taiwan ND temperature BO, the central control year is the year with warm ND, while the NDs before and after the central year are cold. In Fig. 7a we find that the warm

Table 4. The correlation coefficients between the annual average of the normalized anomalies of TAHSLP, AMBO , SCSS and Taiwan ND temperature and JF precipitation during four different periods. The correlation coefficients with asterisks are significant on the 1% level.

		TAHSLP	AMBO	SCSS
Taiwan ND Temperature	*1958-1970*	-0.12	-0.06	-0.04
	1964-1977	-0.36	-0.18	0.14
	1978-1989	**-0.60***	-0.13	-0.19
	1987-1998	-0.49	0.24	0.32
Taiwan JF Precipitation	*1958-1970*	-0.31	0.03	0.09
	1964-1977	-0.18	0.20	0.23
	1978-1989	-0.23	0.04	-0.10
	1987-1998	-0.27	**0.55***	**0.67***

ND0 of Taiwan leads the maximum negative value of TAHSLP that appears in JF+1. After JF+1, TAHSLP anomaly becomes positive in three months. The TAHSLP anomaly reaches its highest value in ND+1. Because the SOI is a more widely used index for monitoring ENSO, we plot the composite SOI in Fig. 7b. The evolution of SOI is almost identical with that of TAHSLP. The smallest standard deviation of both TAHSLP and SOI appears in MJ+1. Both TAHSLP and SOI anomalies reach their lowest value in ND0. The composite result is consistent with the result summarized in Table 2. The probability of a ND in the year before a cold ND to be above normal is larger than to be below normal. This may have resulted from the

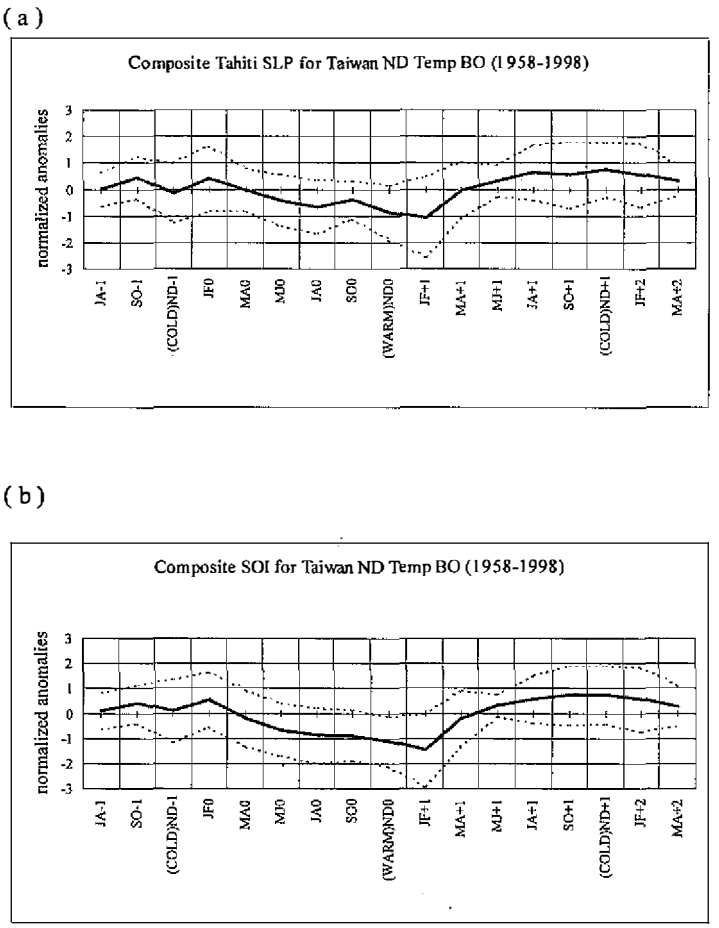

Fig. 7. Sequences of the normalized anomalies in the BO indices of (a) TAHSLP, (b) SOI, (c) Nino4 and (d) SCSS over 7 major BO events of Taiwan Nov-Dec (ND) temperature in 1958-1998. The sequences are from the July-August (JA-1) in the year before the central year of warm ND (ND0) to the March-April (MA+2) in the year after the cold ND (ND+1), which is in the year after the warm ND (ND0). The thick line is the composite mean and the dashed lines are plus and minus one standard deviation.

(c)

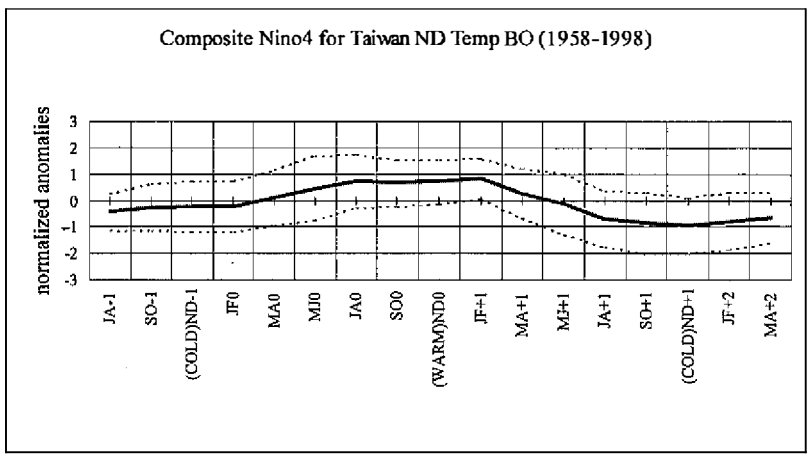

(d)

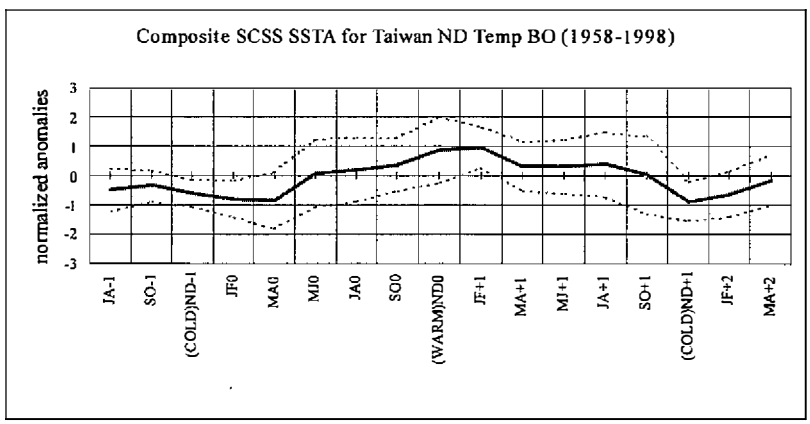

(*Fig. 7.* continued)

modulation of the quick transition of ENSO from the warm phase (negative SOI) to the cold as what Fig. 7b suggests. This relationship is also confirmed in the composite Nino4 shown in Fig. 7c. The standard deviation in Fig. 7c reveals that all selected cases satisfy the condition of changing from the warm to the cold phase of ENSO in the months of from ND0 to MA+2.

Although the correlation coefficient of Taiwan ND temperature and SCS is not high, we find that the composite SCSS (Fig. 7d), on the basis of the BO of Taiwan ND temperature, deserves particular attention. The composite SCSS shows clear coherent biennial fluctuation with respect to Taiwan ND temperature. Within the period of from JA-1 to ND0 in Fig. 7d, we see the phase transition from negative SCSS to the positive in spring (MJ0). The phase transition from the positive to the negative occurs in autumn (SO+1). It seems that the phase transi-

tion from cold Taiwan ND to warm ND is more closely associated with the transition of SCSS, while that from warm Taiwan ND to cold ND is more closely associated with the transition of Nino4 or SOI. It is also noted that the phase transition of SCSS lags behind the transition of Nino4 by about two months. The BO mode of SCSS extracted from the composite analysis and the extracted fast (BO) mode of the ENSO should be considered two aspects in one system, which modulates the fluctuations of Taiwan ND temperature in the biennial time scale.

For the Taiwan JF precipitation, we separate the composite years into two segments of before and after 1982. There are 4 cases in each segment. The separation is based on Fig. 3 that shows that the Taiwan BO signal is stronger after 1982 than before. The contrast of the correlation between Taiwan JF precipitation and the BO indices during different segment of decades as shown in Table 4 is also remarkable. It is also suggested by Table 4 that Taiwan JF precipitation and ENSO are not correlated. However, the precipitation and SCSS and AMBO are significantly correlated in the decade of 1987-1998.

The composite AMBO before 1982 is shown in Fig. 8a. The average anomaly of AMBO is very small in comparison to its standard deviation. This result is consistent with the small correlation between Taiwan JF precipitation and AMBO in Table 4. Figure 8b is the composite SCSS before 1982. Despite of the small anomaly and large standard deviation, a weak positive linear trend can be recognized. Figure 8c shows the composite SOI. A negative trend of SOI from JF-1 to JF+1 can be more clearly identified in Fig. 8c compared with the positive trend in Fig. 8b. The negative trend also appears in the composite IMBO (not shown). The trend may have resulted from the low-frequency mode of ENSO. Nevertheless, the composite results suggest there are no consistent relations between the BO of Taiwan JF precipitation and the BO mode of ENSO.

The composite AMBO after 1982 is shown in Fig. 9a. The systematic difference between the composites before and after 1982 is evident. Although the average AMBO anomaly is small and the standard deviation is large, the coherent biennial oscillations of AMBO and Taiwan JF precipitation are still recognizable. The composite AMBO is negative before MJ-1 and after SO0 but positive in between. This coherent BO can be more clearly seen in the composite SCSS (Fig. 9b). The composite SOI in Fig. 9c shows that during the 17 months of the composite the value of the SOI is mostly negative. However, the negative value is largest in JF0 and the contrast between the three continuous years is still distinguishable. The composite SOI is in sharp contrast to the situation before 1982 as shown in Fig. 8c.

It should be stressed that because BO is not a dominant mode of ENSO, the BO signals emerge in composite results (Figs. 7 and 9) are not trivial and thus are worthy of study. The contrasts between Figs. 8 and 9 suggest that Taiwan JF precipitation BO is more closely related with the biennial scale of the variations in the BO indices, particularly SCSS, after 1982.

5. DISCUSSION

Using spectral analysis technique and the conditional probability approach to analyze 1958-1998 data of 20 Taiwan stations, we have identified two BO modes: the ND temperature and the JF precipitation. Both ND temperature and JF precipitation show clear decadal-scale contrast in the rhythm of their oscillations. There are more biennial oscillations of the ND

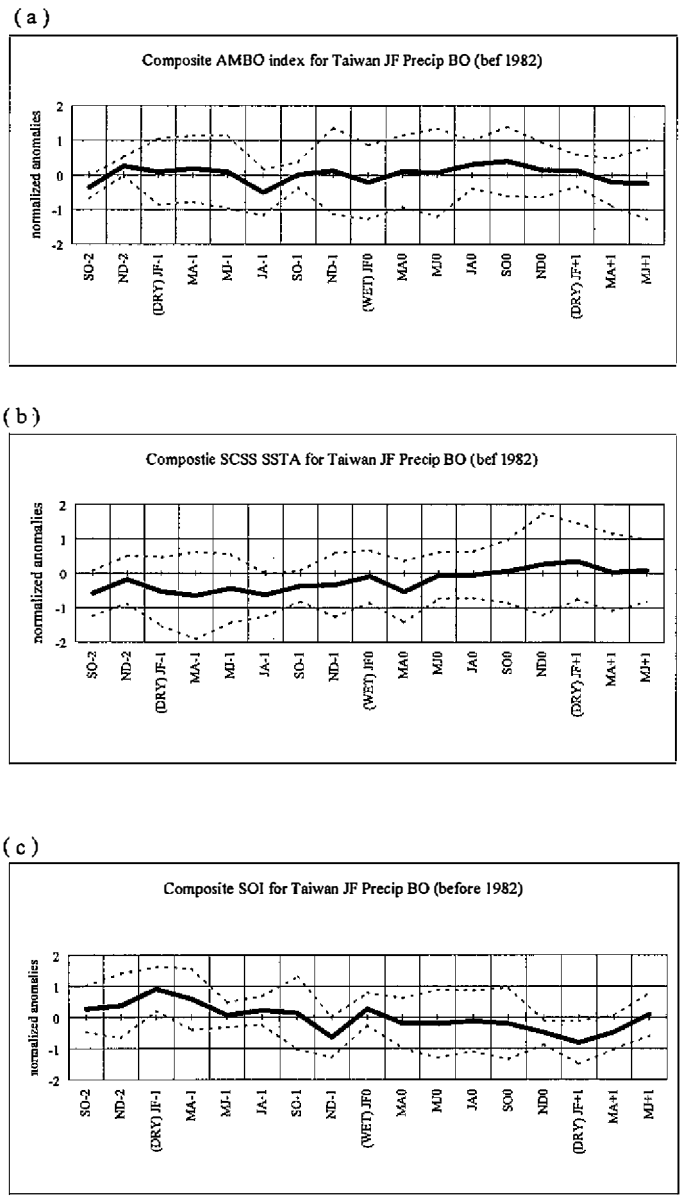

Fig. 8. Sequences of normalized anomalies in the BO indices of (a) AMBO, (b) SCSS, and (c) SOI over 4 major BO events of Taiwan Jan-Feb (JF) precipitation before 1982. The sequences are from the Sep-Oct (SO-2) to the May-June (MJ+1). SO-2 is in the year before the dry JF (JF-1) which is in the year before the central wet JF (JF0). MJ+1 is in the same year of the dry JF (JF+1) which is in the year after the central wet JF (JF0). The thick line is the composite mean and the dashed lines are plus and minus one standard deviation.

(a)

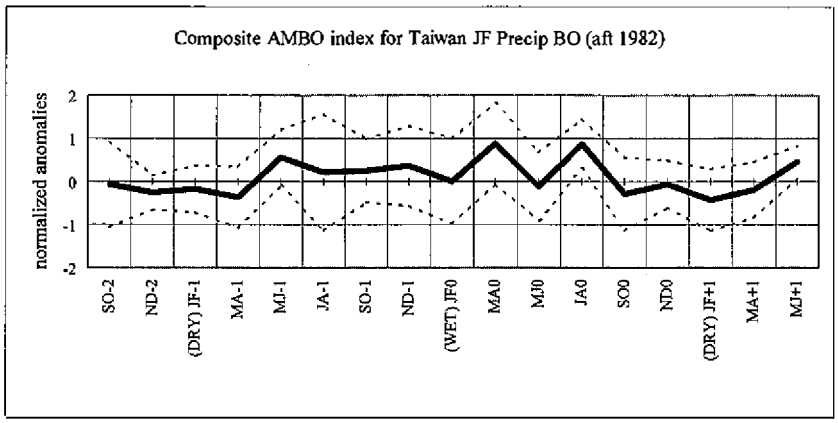

(b)

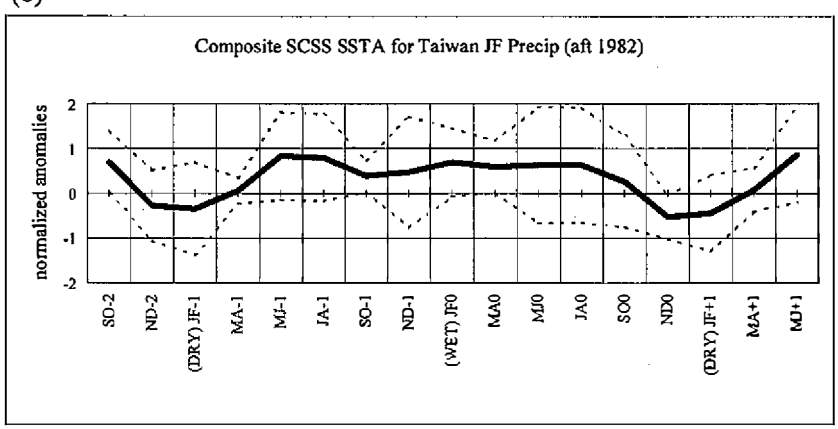

(c)

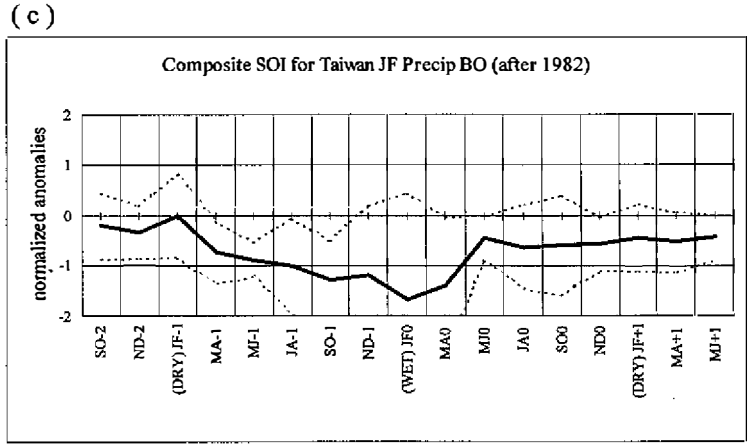

Fig. 9. Same as Fig. 8 but for the events after 1982.

temperature before 1978, but the fluctuation amplitude is smaller than the variations after 1978. The frequency of the dominant interannual fluctuations is lower after 1978. In the contrast, after 1978 the BO mode of JF precipitation is more clearly observed and its amplitude is larger.

Based on certain selected published quasi-biennial oscillation results, we have designed 4 BO indices in addition to the conventional ENSO indices. We find that the BO signal can be best detected in the 41-year monthly indices of TAHSLP, AMBO and SCSS. TAHSLP mainly represents the ENSO activity. AMBO represents extratropical Australian monsoon and SCSS reflects the SST fluctuation in the SCS.

5.1 The ND Temperature

A systematic relationship between the BO modes of Taiwan ND temperature, SCS SST and ENSO is revealed in the composite and correlation analyses. The association is clearer when the ENSO changes from its positive to the negative phase. This finding is consistent with the Taiwan ENSO signal documented in Lu (2000).

In an attempt to understand how Taiwan temperature, SCS SST and ENSO are related, we plot the composite 925hPa wind anomalies in Fig. 10. The composite is based on the same seven events presented in Section 4b and shown in Fig. 7. The cold (warm) anomalies are computed by subtracting the u and v averaged for the category of normal ND from the average values for the cold (warm) ND. Here, the normal refers to those years belong neither to the cold nor to the warm category. The composite results are presented in Figs. 10a, b, and c. The areas in which the significance of the anomalies of either u or v reaches the 90% confidence level are shaded. Focusing on the vicinity of Taiwan, we can see the association of the BO mode of Taiwan ND temperature with the anomalous low-level meridional wind anomalies along the coastal areas of Asian continent from the SCS to the East China Sea. The northerly anomalies are associated with an anticyclone over north China (Figs. 10a and c) and a deep trough from the North Pacific east to Japan extending southwestward to the Philippine Sea. The southerly anomalies near Taiwan in Fig. 10b are associated with an anticyclone over the SCS, which appears as an extension from the North Pacific anticyclone with the center approximately at (25°N, 150°E). The northerly anomalies near Taiwan in Fig. 10c are associated with a trough over the SCS, which is as an extension from the aforementioned deep trough east to Japan.

In the Southern Hemisphere, we notice a large area of westerly anomalies between Australia and the equator in the cold ND before the warm (Fig. 10a). Although the equatorial Pacific Nino4 area (160°E-150°W) is covered by easterly anomalies, they are not significant at the 90% confidence level. A completely different picture is found in Fig. 10b. We see significant westerly anomalies in the Nino4 area and easterly anomalies over the eastern Indian Ocean near the equator and the southern tip of the SCS. A clear contrast in the configurations of the equatorial zonal flow can be identified in the comparison of Figs. 10b and c. Figure 10c bears strong resemblance to Fig. 10a in the Southern Hemisphere and over north China. The westerly anomalies extending from Celebes of Indonesia southeastward to the South Pacific in both figures are striking. The westerly anomalies are part of the anomalous cyclonic

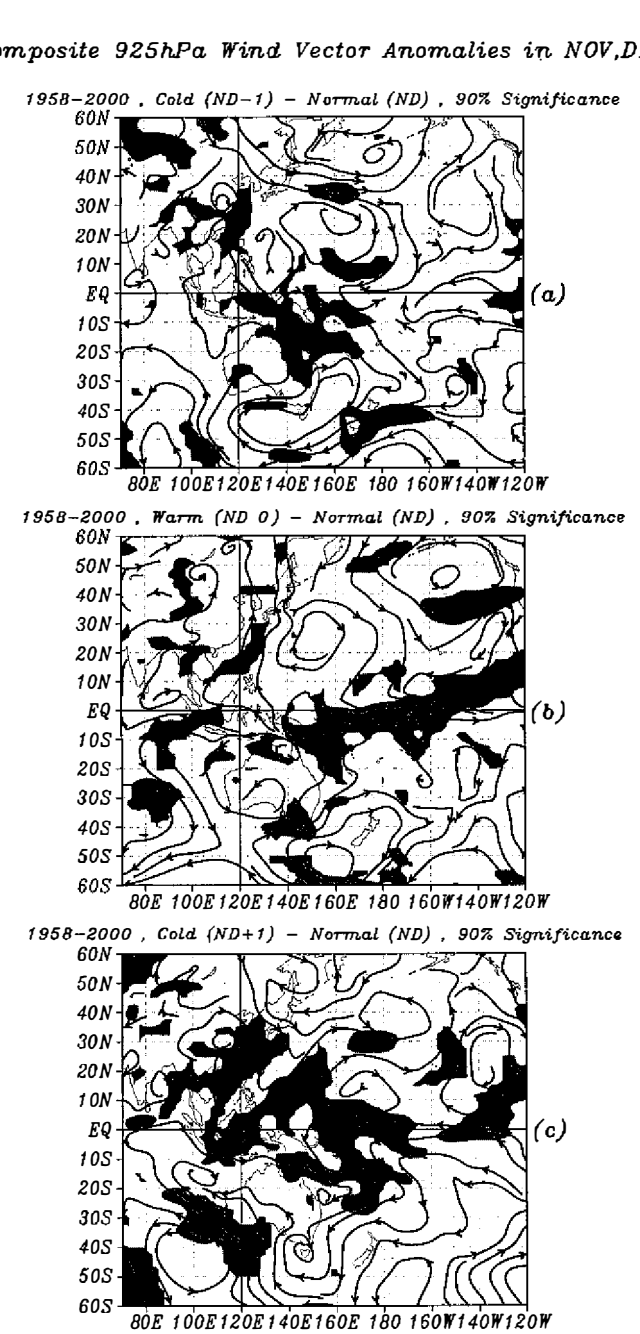

Fig. 10. Composites of the wind anomalies at 925hPa over 7 selected major BO events of Taiwan Nov-Dec (ND) temperature. Detailed description refers to the text. The areas with the composite anomalous u or v significant on 90% level are shaded. The composite is (a) for the cold (ND-1), (b) for the warm (ND0) and (c) for the cold (ND+1).

circulation over or near Australia.

It should be stressed that the composite 925hPa wind fields are in good agreement with the results in Fig. 7 and Table 4, which supports the association of the BO modes of Taiwan ND temperature, SCS SST and ENSO. It is known that the interannual variations of SCS SSTs are modulated by the low-level winds of the East Asian winter monsoon system (Tomita and Yasunari 1996). If we use the circulation dipole with two centers, one over north China and another over SCS, to describe the Taiwan-SCS BO system, then when north China is covered by an anticyclone (cyclone) and the SCS is covered by an cyclone (anticyclone) we say the system is in the northerly (southerly) phase. The northerly phase is associated with the westerly anomalies in the Southern Hemispheric tropics between Australia and the equator. The southerly phase is associated with the westerly anomalies over the equatorial west Pacific and the easterly anomalies over the equatorial eastern Indian Ocean. It is noticed that the biennial oscillations of the large-scale system can be much more clearly identified in the Southern than the Northern Hemisphere. The low-level flow surrounding the Australian continent oscillates coherently with the anomalous equatorial zonal flow and the BO mode of Taiwan ND temperature. These facts are suggestive evidence for a close relationship between the BO modes of Taiwan ND temperature and the atmospheric pressure in the Australian region (Trenberth 1975). Another possible factor driving the Taiwan-SCS BO is the BO mode of ENSO (Barnett 1991; Tomita and Yasunari 1993; Wang et al. 2000). The BO mode of ENSO was stronger before 1978 than after and so was the BO of the SCS SSTs (Fig. 6). The similar regime difference is also found for Taiwan ND temperature (Fig. 3). These results support the possibility that the BO mode of Taiwan ND temperature basically reflects one aspect of the global-scale BO system in which the inter-hemispherical interactions between East Asia and Australia and the associated east-west circulation over the Pacific basin all work together to result in the oscillations.

The spatial and temporal structure of the global-scale BO is depicted in Barnett (1991). The largest BO amplitude appears over Indonesia and Australia in the months of September-November. Such characteristics can be adopted to explain why the BO signals in Taiwan temperature are particularly strong in the season of ND. According to climatology, the inter-hemispherical interactions are most concentrated over the marginal seas from the Yellow Sea to the Timor Sea during the months of ND, before the onset of the Australian summer monsoon. The variations of the interaction have direct impacts on the interannual variability of Taiwan temperature.

The decacal-scale variations of the global-scale BO remain to be studied. The low-level flow patterns shown in Figs. 10a-c suggest that Taiwan BO signal is sensitive to the east-west displacement of the global-scale BO mode. If the East Asia-Australia coupled mode shifts for 10 degrees of longitude to the east, we can imagine that the BO signal of Taiwan ND temperature will be weak. Another interesting point that has not been studied yet is the bimodal structure of the preferred month of the year corresponding to the zero phase of the large-scale BO (Fig. 10 in Barnett 1991). Besides the period of September-November, January-February is the second preferred period in which the BO amplitude over Indonesia and Australia is the largest. The phase of the global-scale BO system can directly affect Taiwan temperature anomalies. It remains to be explored how the modality of global-scale BO mode and Taiwan

BO signals are related in the time scale of climate.

5.2 The JF Precipitation

In contrast to the ND temperature, the BO mode of Taiwan JF precipitation is found to be associated with SCSS only after 1982. The dry JFs of the BO mode are associated with the negative SCS SSTA and the wet JFs are associated with the positive SCS SSTA. It should be noted that the correlation of SCSS and AMBO is significantly high after 1978, but the correlations of SCSS and TAHSLP and of the AMBO and TAHSLP are rather low in the same years. These results lead us to hypothesize that the BO mode of Taiwan JF precipitation is more closely related with the BO signals of SCS SSTA and the cross equatorial flow around Indonesia than ENSO. We will use the composite JF low-level winds, based on the wet and dry phases of Taiwan precipitation and the contrast between the periods before and after 1982 to illustrate the relationship.

We first select 4 wet (1964, 1968, 1972, and 1980) and dry (1963, 1965, 1979, and 1981) years before 1982 according to Fig. 3b. By the same token, we also select 5 wet (1983, 1985, 1990, 1992, and 1994) and dry (1982, 1984, 1989, 1991, and 1993) years after 1982. Then the JF 925hPa wind anomalies are computed with respect to the normal conditions before and after 1982. The normal is computed separately by making the averages of 1958-1981 and 1982-1998 without including the wet and dry years.

The composite 925hPa wind anomalies of the wet (dry) JFs after 1982 are shown in Fig. 11a (Fig. 11b). The significant anomalies in the wet composite are mainly over the longitudinal belt of 100-130°E (Fig. 11a). The southerly anomalies are associated with the anticyclone over the Philippine Sea and the SCS, which has an antisymmetric counter part over Australia. Between these two anticyclones, there are anomalous easterly winds over Indonesia and the eastern Indian Ocean. The anomalous winds over the areas of equatorial Pacific east of the dateline are not significant at the confidence level of 90%, which is in sharp contrast to the wet composite. Figure 11b shows that the areas with significant low-level anomalous winds are mainly over the central Pacific. In the central Pacific, a large area is covered by the anomalous cross-equatorial winds from the Southern Hemisphere. These cross equatorial winds are associated with the anomalous anticyclone extending from Papua New Guinea to Tahiti (18°S, 150°E) in the northwest-southeast orientation. At the southern rim of the anticyclone the wind anomalies are northwesterly. Australia is covered by anomalous anticyclonic circulation in the wet (Fig. 11a), but by cyclonic circulation in the dry (Fig. 11b) composites. The contrast is better depicted in the difference map between the wet and dry (Fig. 11c). The positive correlation between SCSS and AMBO shown in Table 3, the positive correlation between Taiwan JF precipitation and SCSS and AMBO in Table 4, and what we see in Fig. 11c are all consistent. The southerly winds over the SCS are associated with the anticyclonic circulation (high SLP) over Australia and cyclonic circulation (low SLP) over the eastern South Pacific.

The composite wind anomalies before 1982 (Figs. 12a-c) are completely different from the anomalies after 1982. The wet composite (Fig. 12a) shows that the wind anomalies near Taiwan are mainly blowing from the Pacific Ocean and the East China Sea to southeast China at the latitudes of 20-30°N. The dry composite (Fig. 12b) shows the anomalous winds blow

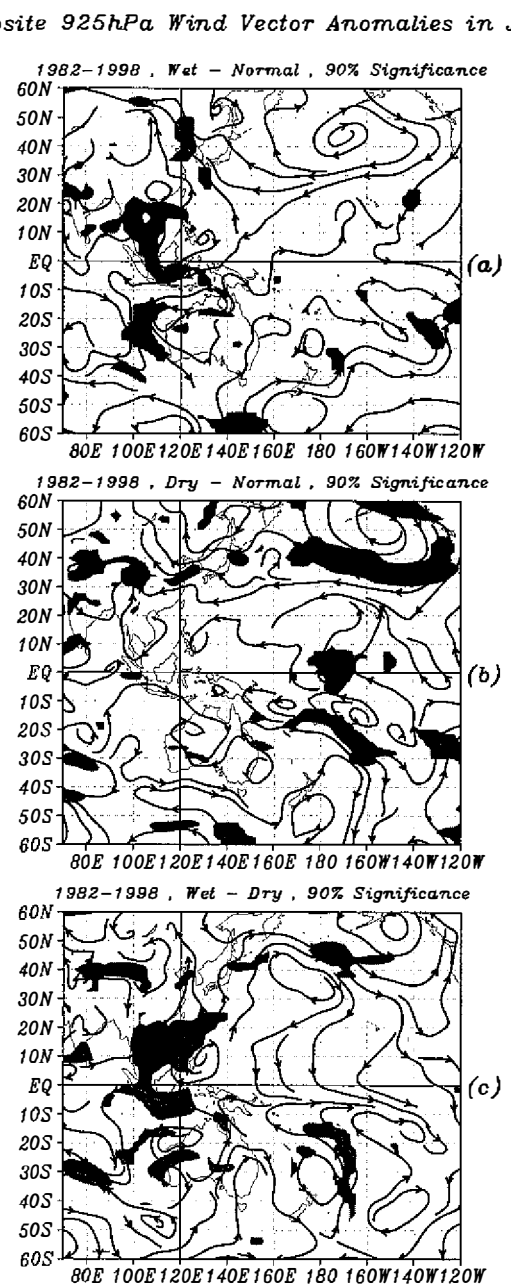

Fig. 11. Composites of the wind anomalies at 925hPa over 4 selected major BO events of Taiwan Jan-Feb (JF) precipitation after 1982. For detailed description, refer to the text. The areas with the difference of u or v significant on 90% are shaded. (a) is the difference between wet and normal, (b) is the difference between dry and normal and (c) is the difference between wet and dry.

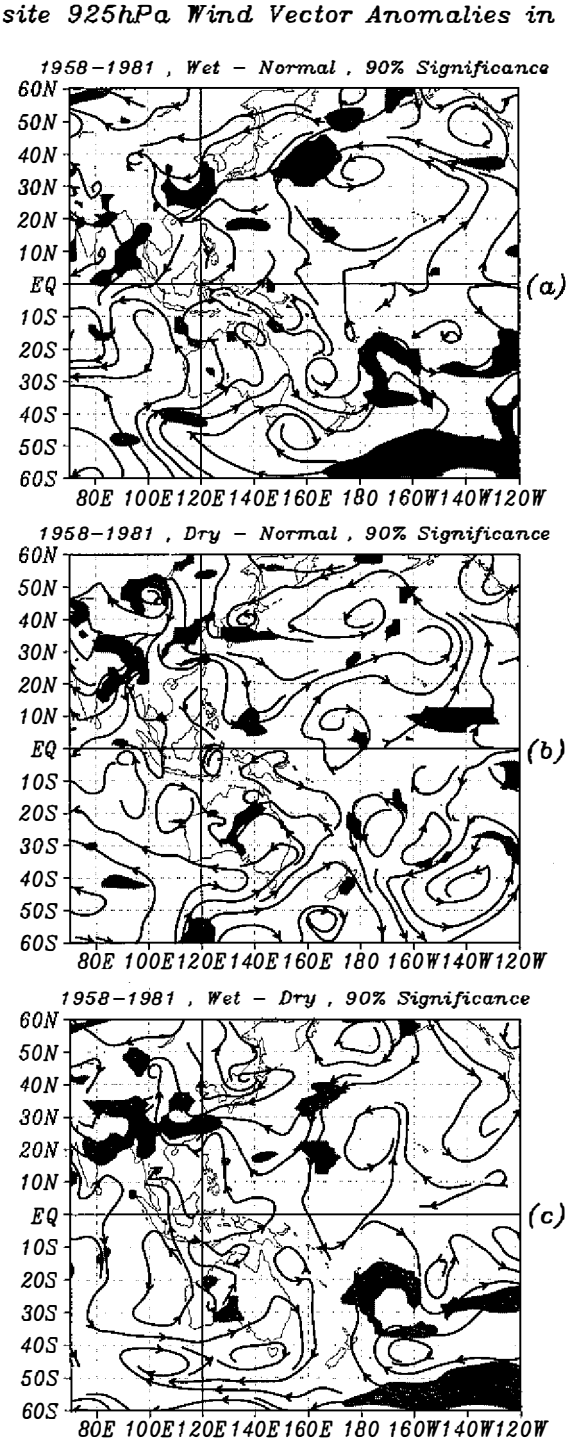

Fig. 12. Same as Fig. 11 but for the four events before 1982.

from the continent to the ocean in the East Asia coastal area near Taiwan. The main difference between the wet and dry composite in the Northern Hemisphere is over Asia, the East China Sea and the North Pacific around 160°E (Fig. 12c). Within the latitudes of 10°N and 10°S, no difference between the wet and dry composites is significant at the 90% confidence level. In contrast to Fig. 12c, Fig. 11c shows a much stronger pair of anticyclones centering over the Philippine Sea and northwest Australia. Significant southerly wind difference over the SCS is observed. Since Taiwan JF precipitation BO is stronger after 1982, this contrast suggests that the tropics may be a key area to look for the origin of the BO signals.

6. CONCLUSIONS

The composite fields of the low-level winds support the robustness of the BO modes of Taiwan ND temperature and JF precipitation. These fields are also in good agreement to the reconstructed quasi-biennial structures of the SLP depicted in Barnett (1991). The phase locking of Taiwan BO modes to the particular seasons of ND and JF may have resulted from the modulation of the phases of the global BO mode by the annual cycle. Generally speaking, if we take the global BO mode as a background "wave", then it should not be hard to find some kind of BO signal within the tropics and subtropics. The BO signal can exceed other kinds of interannual variability only if it is favored by the annual cycle at that particular location. Taiwan BO signals can be reasonably interpreted in such a scenario.

The Taiwan BO modes manifest one aspect of tropical-extratropical interactions along the north-south elongated region from Australia to north China and Japan. The ND temperature mode is more clearly observed before the late-1970s in which the BO signal of the JF precipitation is less evident. The discrepancy between temperature and precipitation signals may be due to the rapid warming trend of SCS SSTs (Fig. 6) and the Eurasia continent (Diaz and Baradley 1995) in late-1970s. The warm SSTs can increase the moisture in the boundary layer of the atmosphere, thus increasing the precipitation in Taiwan, particularly when the anomalous winds over the SCS are southerly. The anomalous southerly winds are usually associated with an anomalous anticyclone extending from the western Pacific to south SCS (Wang et al. 2000). On the other hand, when the Eurasia continent becomes warmer than normal, the winter continental anticyclone over north China weakens. Therefore, the warm anomalies of the continental temperature and SSTs can mask the negative phases of the BO mode of Taiwan ND temperature. This explains why the BO mode of Taiwan temperature is weaker after the late-1970s. Therefore, our results suggest that the BO mode of Taiwan JF precipitation mainly results from the global BO mode, the BO mode of ENSO on top of the warm SCS SSTs, while the BO of ND temperature results from a delicate relationship of the tropical-extratropical interactions modulated by the global BO mode.

Acknowledgements The work is supported by the CWB/ Meteorological Research Development Center Climate Project and NSC (National Science Council of Taiwan) grant NSC89-2621-Z-052-001. The monthly NCEP/NCAR Reanalysis and Kaplan extended SST anomaly data were obtained from the data library of the IRI (International Research Institute for climate prediction) from their Web site at http://iri.ldeo.columbia.edu. The SOI data were obtained

from NOAA-NCEP Climate Prediction Center from their Web site at http://www.cpc.noaa.gov. Special thanks to Professor Chi-Pei Chang for stimulating discussion, and to Professor Michio Yanai for motivating this study by creating an electronic TBO discussion session. The author would like to express her appreciation to two anonymous reviewers whose comments greatly improved the contents of this paper.

REFERENCES

Barnett, T. P., 1991: The interaction of multiple time scales in the torpical climate system. *J. Climate*, **4**, 269-285.

Brier, G. W., 1978: The quasi-biennial oscillation and feedback processes in the atmosphere-ocean-earth system. *Mon. Wea. Rev.*, **106**, 938-946.

Chang, C. P., and T. Li, 2000: A theory for the tropical tropospheric biennial oscillation. *J. Atmos. Sci.*, **57**, 2209-2224.

Diaz, H. F., and R. S. Bradley, 1995: Documenting natural climatic variations: How different is the climate of the twentieth century from that of previous centuries? *Natural Climate Variability on Decade-to-Century Time Scales*, National Research Council, 17-29.

Kalnay, E., and Cosuthors, 1996: The NCEP/NCAR 40-Year Reanalysis Project. *Bull. Amer. Meteor. Soc.*, **77**, 437-471.

Lu, M.-M., 2000: Taiwan abnormal climate and ENSO. *Atmos. Sci.*, **28**, 91-114. (in Chinese)

Meehl, G., 1987: The annual cycle and interannual variability in the tropical Pacific and Indian Ocean regions. *Mon. Wea. Rev.*, **115**, 27-50.

Meehl, G., 1997: The south Asian monsoon and the tropospheric biennial oscillation. *J. Climate*, **10**, 1921-1943.

Nicholls, N., 1978: Air-sea interaction and the Quasi-Biennial Oscillations. *Mon. Wea. Rev.*, **109**, 1505-1508.

Rasmusson, E. M., S. Wang, and C. F. Ropelewski, 1990: The biennial component of ENSO variability. *J. Mar. Sci.*, **1**, 71-96.

Ropelewski, C. F., M. S. Halpert, and X. Wang 1992: Observed tropospheric biennial variability and its relationship to the Southern Oscillation. *J. Climate*, **5**, 594-614.

Shen, S., and K. M. Lau, 1995: Biennial oscillation associated with the east Asian summer monsoon and tropical sea surface temperatures. *J. Meteor. Soc. Japan*, **73**, 105-124.

Terray, P., 1995: Space-time structure of monsoon interannual variability. *J. Climate*, **8**, 2595-2619.

Tomita, T., and T. Yasunari, 1993: On the two types of ENSO. *J. Meteor. Soc. Japan*, **2**, 273-284.

Tomita, T., 1996: Role of the northeast winter monsoon on the biennial oscillation of the ENSO/Monsoon system. *J. Meteor. Soc. Japan*, **74**, 399-413.

Trenberth, K. E., 1975: A quasi-biennial standing wave in the Southern Hemisphere and interrelations with sea surface temperature. *Quart. J. R. Met. Soc.*, **101**, 55-74.

Trenberth, K. E., 1980: Atmospheric quasi-biennial oscillations. *Mon. Wea. Rev.*, **108**, 1370-

1377.

Troup, A. J., 1965: The Southern Oscillation. *Quart. J. R. Met. Soc.*, **91**, 490-506.

Yasunari, T., 1987: Global structure of the El NiZo/ Southern Oscillation . Part II. Time evolution. *J. Meteor. Soc. Japan*, **65**, 81-102.

Wang, B., R. Wu, and X. Fu, 2000: Pacific-East Asian teleconnection: How does ENSO affect East Asian Climate? *J. Climate*, **13**, 1517-1536.